Phys Chem Minerals (2003) 30: 503–510
DOI 10.1007/s00269-003-0349-8

ORIGINAL PAPER

C. Ferraris · L. Folco · M. Mellini

Sigmoidal exsolution by internal shear stress in pyroxenes from chondritic meteorites

Received: 31 January 2003 / Accepted: 1 July 2003

Abstract Pyroxenes of pigeonitic and augitic bulk compositions in H3–4 chondritic meteorites commonly exhibit sigmoidal precipitates, rather than the elsewhere common lamellar associations. Most often, submicrometric sigmoids with calcic clinopyroxene composition occur within clinoenstatite; more rarely, clinoenstatite sigmoids occur within calcic clinopyroxene. The sigmoids appear as '001' terminated lamellae, with terminations rotated in opposite directions towards the '100' orientation. Pre-exsolution pigeonite and augite formed at temperatures higher than 980 °C, whereas sigmoidal exsolution occurred between 990 and 830 °C. Local anomalous lattice parameters determined by electron diffraction suggest that lattice parameters are most strained where the exsolution texture is most poorly defined. Shear strain occurs during exsolution due to mismatching lattice parameters and variable β angles. In response to shear stress, the lamellae relax and assume sigmoidal strained morphologies. Sigmoidal exsolution is strongly controlled by (100) orthoenstatite stacking faults that possibly trigger exsolution.

Keywords Exsolution · Pyroxene · Chondrule · Sigmoids · Shear stress

Introduction

Exsolution features are common in different minerals. They result from phase transitions when a homogeneous solid solution, stable at high temperatures (HT), exsolves into two compositionally different phases during cooling. The low temperature (LT) phases may have common structures, or may differ in symmetry and local site distortions (e.g. Putnis 1992). For instance, the exsolution from HT subcalcic pyroxenes with $C2/c$ symmetry may result in $C2/c$ calcic pyroxenes plus $Pbca$, or $P2_1/c$ iron and magnesium pyroxene intergrowths. As exsolution is thermodynamically controlled, reliable geothermometers are based on ion exchange amongst coprecipitates. An example is the two-pyroxene geothermometer calibrated by Lindsley (1983).

Exsolution requires atomic diffusion through the crystal. The corresponding activation energy is high (e.g. 99 kcal mol^{-1} for Fe-free clinopyroxene; McCallister 1978), with reaction kinetics slow enough to determine two consequences. Firstly, the HT phase may survive cooling (which prevents the attainment of chemical equilibrium throughout the crystal) if cooling is fast enough. Secondly, exsolution may produce finely intermixed products rather than completely segregated ones. Given that exsolution is kinetically controlled, several geospeedometers are based on such microstructural data. A recent example is the study of exsolution and coarsening of lamellar precipitates in synthetic clinopyroxenes (Weinbruch et al. 2001).

While studying pyroxene microstructures and cooling history in H3 chondritic meteorites (Ferraris et al. 2002), we systematically observed texturally anomalous features, i.e. sigmoidal domains, rather than the usual lamellar associations or spinodal pseudo-periodic oscillations commonly found in terrestrial and extraterrestrial pyroxenes.

In this work we have reexamined the pyroxenes from the chondrules described in Ferraris et al. (2002) and conducted new TEM-AEM observations on additional samples from H3 and H4 chondrites, focusing on phase relationship and geometry of the sigmoidal precipitates. The specific aim of this work is to compare their presence in chondritic meteorites with other occurrences in natural rocks and synthetic products, and discuss the

C. Ferraris · M. Mellini (✉)
Dipartimento di Scienze della Terra,
Università di Siena, Via Laterina 8, 53100 Siena, Italy
e-mail: mellini@unisi.it

C. Ferraris
Institute of Environmental Science Engineering,
Nanyang Technological University, Innovation Centre Block 2,
Unit 247, 18 Nanyang Drive, Singapore 637723

L. Folco
Museo Nazionale dell'Antartide, Università di Siena,
Via Laterina 8, 53100 Siena, Italy

physico-chemical constraints controlling their development.

Experimental

We studied ten samples from nine different chondrules from four H3 and H4 chondritic meteorites (FRO 90003, FRO 90032, Brownfield and Raguli). Abbreviations of the meteorite names (i.e. FR3, FR32, BFR and RAG), followed by a progressive number, are used to indicate the various chondrule samples from the four meteorites. Eight chondrules (BFR-18, FR3-4, FR3-2, FR3-1, BFR-14, BFR-8, BFR-6/2 and FR32-2) are described in detail by Ferraris et al. (2002). The ninth chondrule, RAG-20, was extracted from the Raguli H4 chondrite (Folco et al. 1996; Folco 1997); the tenth sample, BFR-6/1, is one more BFR6 subsample. All chondrules (Table 1) are chemically classified as type II, FeO-rich chondrules (A and B notations are used for olivine- and pyroxene-rich chondrules, respectively; Grossman et al. 1988; Brearley and Jones 1998) and texturally described as POP (porphyritic olivine and pyroxene), C (cryptocrystalline), RP (radial pyroxene) and BP (barred pyroxene) following Gooding and Keil (1981). Details of sample preparation and electron microscopy are given by Ferraris et al. (2002).

Electron diffraction was calibrated repeatedly using external standards. Lattice parameters were determined repeatedly to check the hysteresis of electromagnetic lenses, obtaining values accurate to less than $\pm 1\%$ relative.

Results

All chondrules are characterized by abundant enstatite crystals. Their cores consist of variably faulted orthoenstatite (OREN) and clinoenstatite (CLEN) lamellar associations. The cores are mantled by pigeonitic (PIG) or, less frequently, augitic rims. Rims are a few micrometres thick and show exsolved textures with sigmoidal geometry. The most common situation is given by exsolved pigeonite rims, where well-formed Ca-rich augitic sigmoidal precipitates occur within a Ca-poor matrix. The opposite situation, namely Ca-poor precipitates hosted within Ca-rich clinopyroxene matrix, was observed less frequently in exsolved augitic rims. In the latter case, the sigmoidal shape is sometimes less evident. Data, including chondrule-type TEM-EDS pyroxene chemical compositions and geothermometric estimates (crystallization and exsolution temperatures), are summarized in Table 1; lattice parameters of the exsolved phases are given in Table 2.

In the following paragraphs we report TEM-AEM observations from RAG-20, FR3-1 and BFR6-1 as exemplifying samples of the actual exsolution textures occurring in pyroxene from type-3 and type-4 ordinary chondritic meteorites. Additional data regarding texture, microstructures and mineral composition of the studied samples can be found in Ferraris et al. (2002).

Exsolved pigeonites

RAG-20

Figure 1a is an [010] electron image showing the arrangement of low-Ca pyroxenes in a Raguli radial pyroxene chondrule. The field on the right (as well as the small field top left) consists of almost homogeneous orthoenstatite (OREN) domains, faulted by a few (100) CLEN lamellae. The central portion of the picture corresponds to a (100) pigeonite lamella (PIG), approximately 1 μm thick, exsolved into horizontal CPX and CLEN lamellae. Phase identification was based on chemical composition (Table 1) and electron diffraction patterns (one from a $C2/c$ CPX with $h = 2n$ spots in the $h0l$ plane and another from a $P2_1/c$ CLEN with spots for both even and odd h values). The average thicknesses of CPX and CLEN are, respectively, 70 and 260 nm, i.e. about 1 order of magnitude thicker than in H3 chondrites (see below, and Ferraris et al. 2002). Careful inspection of Fig. 1a reveals that these CPX and CLEN lamellae are not arranged in a regular pattern: their thickness varies and they are not exactly parallel to one another. Furthermore, the CPX–CLEN interfaces only approximate the (001) crystallographic planes. The CPX and CLEN lamellae will therefore be indicated as '001' lamellae, following the convention used by Robinson et al. (1971) to indicate the approximate crystallographic

Table 1 TEM-EDS compositions of sigmoidal exsolution textures, and estimated temperatures

Sample	Chondrule type	Bulk composition	Matrix composition	Precipitate composition	Minimal crystallization temperature (°C)	Exsolution temperature (°C)[a]
RAG-20	RP	En_{75} Wo_{9} Fs_{16}	En_{84} Wo_{1} Fs_{15}	En_{59} Wo_{33} Fs_{8}	1030	870 ± 50
BFR-18	POP	En_{72} Wo_{10} Fs_{18}	En_{77} Wo_{1} Fs_{22}	En_{55} Wo_{35} Fs_{10}	1020	830 ± 60
FR3-4	BP	En_{66} Wo_{17} Fs_{17}	En_{72} Wo_{11} Fs_{17}	En_{52} Wo_{43} Fs_{5}	1070	[b]
FR3-2	C IIAB	En_{67} Wo_{14} Fs_{19}	En_{74} Wo_{3} Fs_{23}	En_{45} Wo_{45} Fs_{10}	1020	970 ± 50
FR3-1	C IIAB	En_{63} Wo_{13} Fs_{24}	En_{70} Wo_{3} Fs_{27}	En_{41} Wo_{44} Fs_{15}	980	980 ± 70
BFR-14	RP	En_{67} Wo_{17} Fs_{16}	En_{72} Wo_{5} Fs_{23}	En_{53} Wo_{31} Fs_{16}	1070	[b]
BFR-8	POP	En_{74} Wo_{12} Fs_{14}	En_{80} Wo_{2} Fs_{18}	En_{58} Wo_{31} Fs_{11}	1030	990 ± 40
BFR-6/2	C IIAB	En_{72} Wo_{12} Fs_{16}	En_{79} Wo_{2} Fs_{17}	En_{52} Wo_{37} Fs_{11}	1020	980 ± 25
BFR-6/1	C IIAB	En_{57} Wo_{29} Fs_{14}	En_{58} Wo_{35} Fs_{8}	En_{80} Wo_{2} Fs_{17}	1210	980 ± 130
FR32-2	RP	En_{63} Wo_{36} Fs_{1}	En_{53} Wo_{44} Fs_{3}	En_{93} Wo_{1} Fs_{6}	1240	900 ± 40

[a] T calculated for cpx–opx pairs in the QUILF program
[b] T not calculated because of contaminated analyses

Table 2 Unit-cell parameters obtained by electron diffraction

Chondrite	Pyroxenes	β (°)	a (nm)	c (nm)
RAG-20	CPX	105.3	0.975	0.525
	CLEN	107.5	0.961	0.524
BFR-18	CPX	105.2	0.974	0.525
	CLEN	107.7	0.967	0.522
FR3-2	CPX	104.9	0.978	0.524
	CLEN	107.4	0.970	0.523
FR3-1	CPX	104.5	0.974	0.525
	CLEN	107.4	0.969	0.524
BFR-6/2	CPX	105.6	0.978	0.533
	CLEN	108.6	0.971	0.532
BFR-6/1	CPX	105.4	0.955	0.536
	CLEN	108.4	0.934	0.536
FR32-2	CPX	105.5	0.947	0.532
	CLEN	108.3	0.933	0.532

orientation of a lamella; in this case, the lamellae deviate by ~10° with respect to (001).

Figure 1b reports another example of sigmoidal exsolution features from RAG-20 to highlight the constant appearance, size and shape of the precipitates within the same chondrule. The smaller CPX lamella and the larger CLEN lamella assume a sigmoidal, S-shaped contour. The sigmoidal shape may be described in terms of lamella rotation. Namely, the '001' interfaces progressively rotate towards the '100' interface marked by the (100) OREN-PIG interface, with an angle of ~ 15° between '100' and (100).

The microstructural detail of the CLEN–CPX interfaces may be observed in Fig. 1c and d, which shows the lamellar arrangement in the hook-like region [tip of the lamella close to the (100) OREN–PIG interface]. Non-stepped, continuous and smoothed surfaces separate CPX from CLEN. Owing to the different systematic extinctions, CLEN produces 0.9-nm lattice fringes, whereas the smaller CPX lamella produces 0.45-nm lattice fringes. In particular (Fig. 1d), we observe two sharp kinks in the lattice fringe sequence of the CLEN–CPX interfaces; at the interface, the $h00$ lattice fringes rotate 2.2°, as required by the different values of the β angles in CLEN and CPX (107.5° and 105.3°, respectively, as measured in the

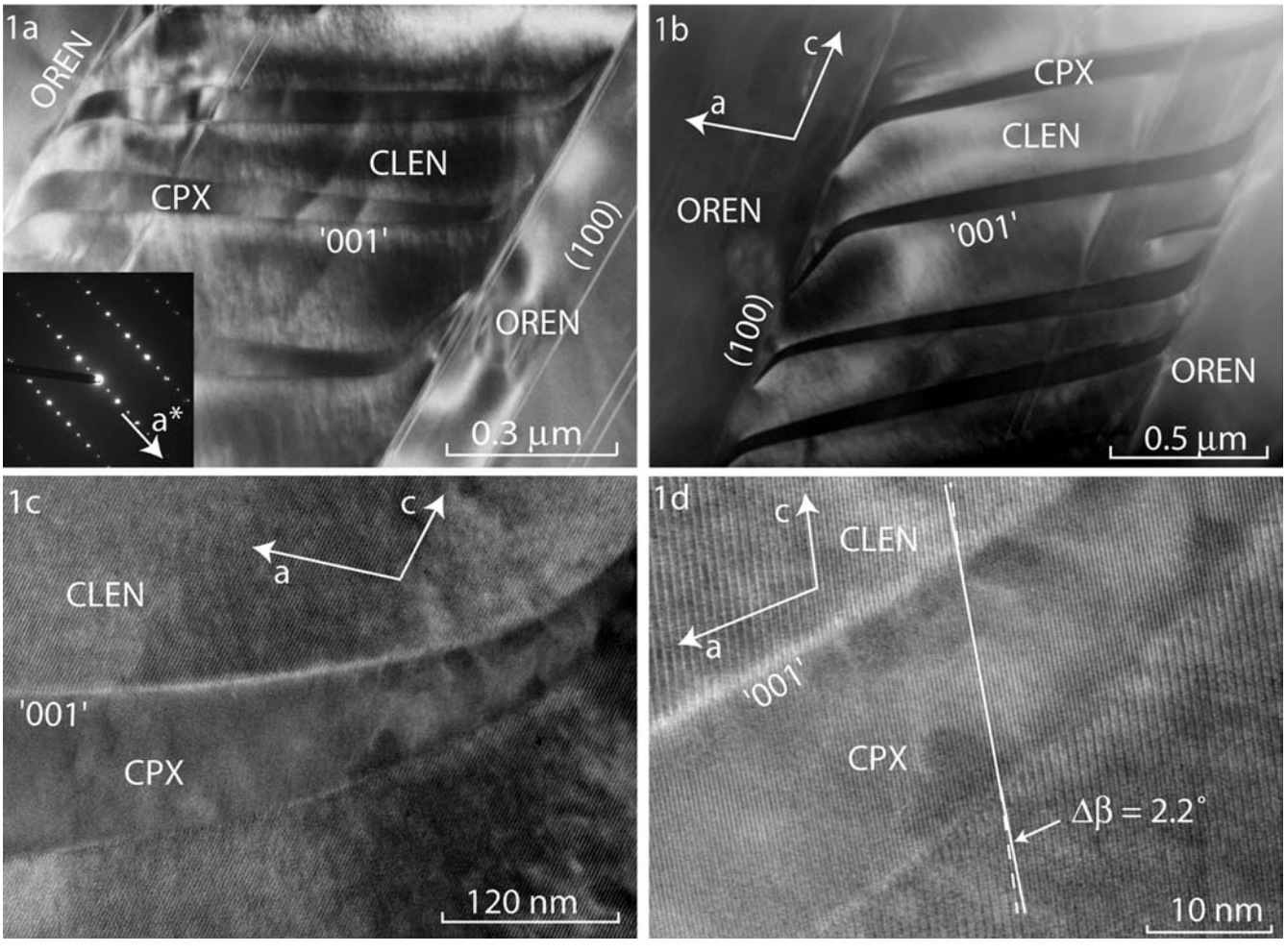

Fig. 1a–d Complex phase relationships among pyroxenes in the RAG-20 chondrule. **a** An OREN matrix with (100) CLEN stacking faults is cut by a (100) pigeonite lamella, now exsolved into '001' CPX and CLEN sigmoids. CLEN and CPX display internal contrast features nearly parallel to (100). *Inset*: SAED pattern. **b** '001' CPX and CLEN sigmoids, formed by exsolution of a primitive (*100*) pigeonite lamella. **c** '001' CPX sigmoids are separated from '001' CLEN sigmoids through non-stepped, smoothed interfaces. **d** $h00$ lattice fringes abruptly tilt by 2.2° through CLEN–CPX interfaces

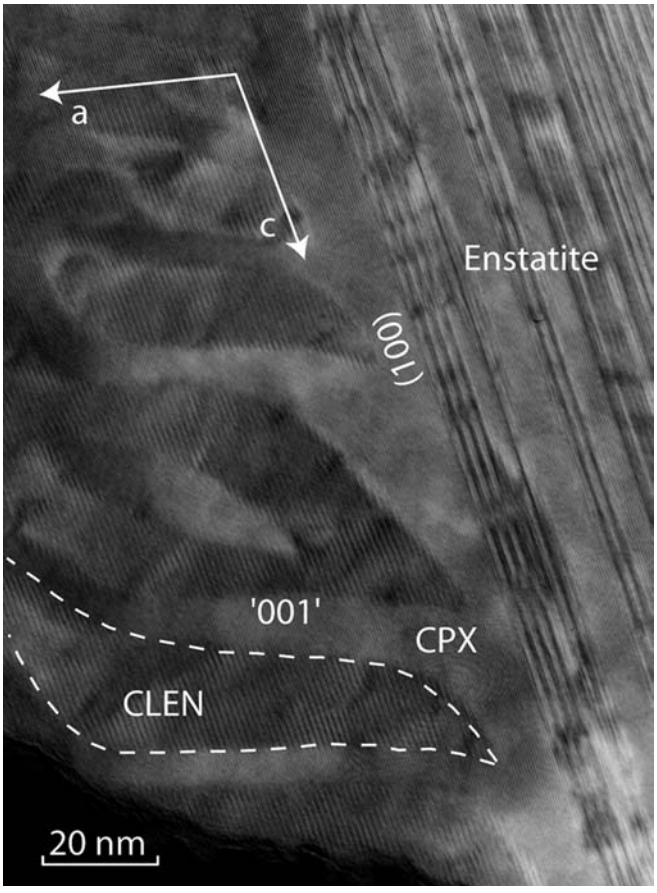

Fig. 2 Complex pyroxene relationships within the FR3–1 chondrule. The faulted enstatite core (*right*) is rimmed by pigeonite (*left*) exsolved into CPX and CLEN sigmoids

SAED). Also unit cell translations (Table 2) differ, being $a = 0.975$ nm and $c = 0.525$ nm for CPX, and $a = 0.961$ nm and $c = 0.524$ nm for CLEN. Namely, rather than completely coherent, the CLEN–CPX interface appears to be semicoherent.

The two-pyroxene geothermometer (Lindsley 1983) was applied to different CPX–CLEN pairs, yielding exsolution temperatures of 870 ± 50 °C (Table 1). This value is consistently lower than the minimal crystallization temperature of 1030 °C estimated for the bulk pre-exsolution pigeonite (i.e. CPX + CLEN), using the same thermometer in the one-pyroxene approximation.

FR3–1

This is a cryptocrystalline IIAB chondrule characterized by microstructures very similar to those occurring in FR3–2, from the same chondrite (Ferraris et al. 2002). The highly faulted OREN + CLEN core is surrounded by a pigeonitic rim, which is exsolved into CLEN and CPX domains with pronounced sigmoidal shapes (Fig. 2). The exsolution products are typically close to 20 nm thick. '001' is the most developed phase boundary, forming an angle close to 7° with respect to (001).

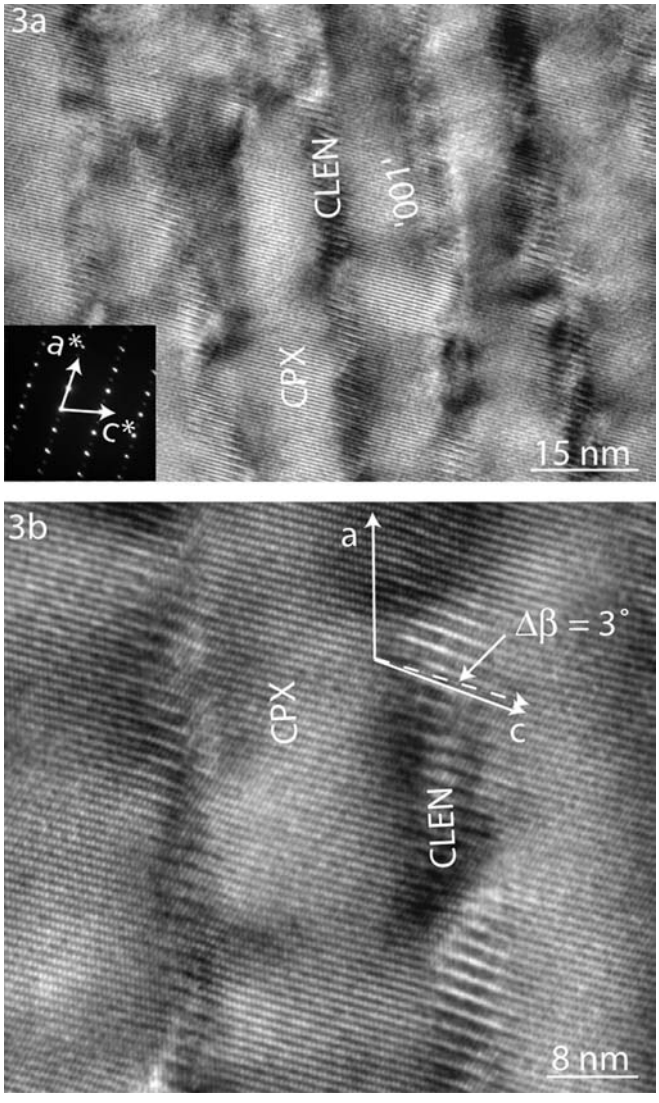

Fig. 3a,b Exsolution texture in the augitic rim of the BFR-6/1 chondrule. **a** The matrix consists of CLEN separated from exsolved CPX through fluctuating '001' boundaries. **b** Evident kinking of *h*00 lattice fringes across the contact plane between CPX and CLEN

As previously seen for RAG-20, the '001' boundary rotates towards '100', forming a 20° angle with respect to (100). Kinking of lattice fringes is evident, with a β angle of 107.4° in CLEN and of 104.5° in CPX. The other cell parameters (Table 2) are $a = 0.974$ nm and $c = 0.525$ nm for CPX, and $a = 0.969$ nm and $c = 0.524$ nm for CLEN. Temperatures are close to 980 °C for both crystallization of the bulk rim and CLEN–CPX intergrowths (Table 1).

Exsolved CPXs

BFR-6/1

In this cryptocrystalline chondrule, the OREN/CLEN core is sporadically surrounded by a CPX rim. This rim

is also separated from the core by a sharply defined (100) plane. The rim (Fig. 3a) has subcalcic CPX bulk composition (Table 1), but consists of a fine association of CLEN domains (0.9-nm periodicity) dispersed throughout the calcic CPX matrix (0.45-nm periodicity).

The '001' interfaces between the CPX matrix and CLEN have variable orientations. In particular, Fig. 3b shows that the apparent '001' CLEN lamella actually consists of several subdomains forming different angles with respect to (001).

Once more, there is evident kinking of (100) lattice fringes at the CPX–CLEN semi-coherent interface, ($a = 0.955$ nm, $c = 0.536$ nm and $\beta = 105.4°$, and $a = 0.934$ nm, $c = 0.536$ nm and $\beta = 108.4°$ for CPX and CLEN, respectively; Table 2).

Geothermometric estimates yielded minimal crystallization temperatures of 1210 °C, followed by lower exsolution temperatures of 980 ± 130 °C (Table 1).

Discussion

Occurrence of sigmoids

Although features akin to those previously described for chondritic meteorites have been reported in several papers (see below), their geometries and origin have never been thoroughly investigated.

What we have called sigmoidal precipitates (or, in short, sigmoids) were first reported in the early 1980s in both terrestrial and extraterrestrial rocks (achondritic meteorites). Kitamura et al. (1981a) studied exsolved augite from the Bushveld gabbro and found laterally terminated (001) lamellae with tips bent from '001' towards the '100' orientation (e.g. their Figs. 1 and 2). The change in morphology was interpreted to occur during cooling as a way of reducing strain at the interface. Kitamura et al. (1981a) used the "morphology change temperature (MCT)" to take into account the best fit of exsolution lamellae into the pyroxene structure, with the '001' and '100' planes favoured by temperatures respectively higher or lower than the MCT, in agreement with the "optimal phase boundaries" theory of Robinson et al. (1971). The same authors (Kitamura et al. 1981b) further explained the change of the interface morphology between '001' pigeonite lamella and augite host as due to late transformation of pigeonite into augite and hypersthene.

Similarly, Takeda et al. (1981) found sigmoidal shapes in the Moore County cumulate eucrite (e.g. their Fig. 5), and reported that "(001) augite lamellae tend to elongate and form short slabs of augite with (100) in common with the host orthopyroxene". They inferred a final temperature of 850 °C for the development of the lamellae, in agreement with our determinations.

Rietmeijer and Champness (1982), while studying the complex cooling history of the Bjerkrein–Sokndal lopolith, observed a change from '001' to '100' in the habit plane of pigeonite lamellae (e.g. the so-called PII in their Fig. 4a) close to the OII orthopyroxene lamella. Following Robinson et al. (1977), they calculated the orientation of the '100' and '001' lamellae as a function of temperature using modeled cell parameters appropriate to the strain-free solvus, and proposed that the PII lamellae nucleated between about 600 and 400 °C.

Feuer et al. (1991) report monzodioritic augites hosting (001) augite lamellae that "change their habit plane from '001' to '100' at their tips". In some cases, the lamellae change their orientation up to 11 times, developing a sinuous, serpentine shape (e.g. their Fig. 6.5).

The only report of sigmoidal exsolutions in meteoritic pyroxene is given by Müller (1993), who observed very fine (the actual dimensions are unspecified, but they are

Fig. 4 TEM images and sketch of strained interfaces between exsolved sigmoids and matrices. The sigmoidal shape is due to shear stress induced by differences in cell parameters and in the β angle between CLEN and CPX

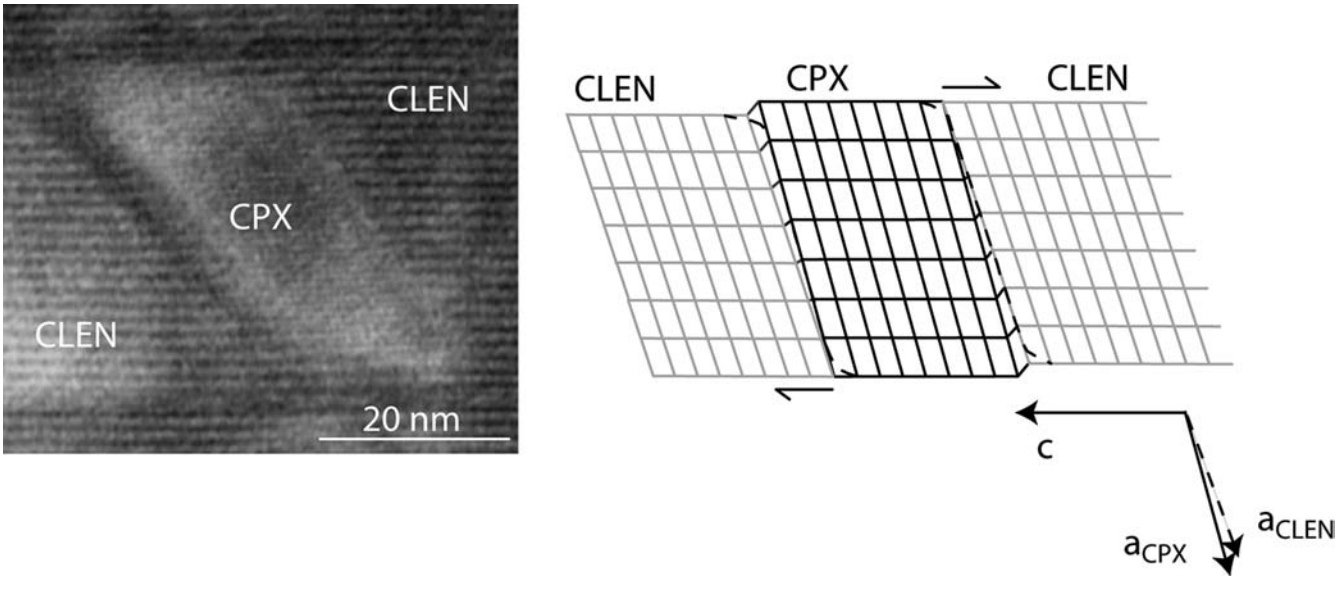

surely $\ll 0.5$ μm as derived from photographs), second-generation S-shaped precipitates of augitic composition in exsolved pigeonites of the Shergotty martian meteorite. In particular, sets of S-shaped precipitates are confined in between antiphase domains (APD) with preferential orientation of the antiphase boundaries (APB) parallel to about (3 0 $\bar{1}$). As APBs form during the high ($C2/c$) to low ($P2_1/c$) pigeonite transformation, Müller (1993) thus mentioned that the sigmoids also likely formed after inversion of the host pigeonite, with APBs acting as sites for heterogeneous nucleation of the precipitates. Based on a direct comparison with microstructures observed in a well-constrained natural system, i.e. the Whin Sill in northern England, cooling rates in the order of 10^{-3} °C hr^{-1} in the 1100–800 °C temperature range were inferred.

More recently, sigmoidal shapes have been reported in the pyroxenes from the tholeiitic sill of the Englewood Cliffs section of the Palisade Sill (Fig. 1b in Moore et al. 2001a), and in the Victoria Valley sill of the Ferrar dolerites (Fig. 10 in Moore et al. 2001b), and appear on the front cover of the volume Solid solutions in silicate and oxide systems (Geiger 2001).

Synthetic pyroxenes may also contain sigmoidal precipitates. Ried and Fuess (1986) synthesized different pyroxenes, with wollastonite contents in the 20–27 mole % range. Specimens tempered at about 870 °C (e.g. the ones in their Fig. 2c and d) showed pigeonites with diffuse interfaces similar to the worm-like sigmoids occurring, for instance, in our FR3-4 (Ferraris et al. 2002). Feuer et al. (1989), studying exsolution products in synthetic pigeonites, observed '001' ''augite-like platelets with a distinct S-shaped morphology'', approximately 6×50 nm in size (e.g. their Fig. 2, not unlike our Fig. 1d), which produced lattice fringes kinked at the interface by 2.5°, with a morphology probably governed by strain energy.

Exsolution products, which change their habit from '001' to '100' lamellae, are common in many different pyroxenes. In most cases, '001' develops between CPX and PIG, or between CPX and CLEN; in contrast, the presence of an OREN (100) lamella induces the CPX and CLEN '001' lamellae to bend towards the '100' shape. The basic crystallographic theory, which explains this behaviour, is well established (Robinson et al. 1971, 1977). Most authors (e.g. Takeda et al. 1981; Ried and Fuess 1986) refer this event to temperatures of 850–870 °C.

From this overview of the occurrence of sigmoidal exsolutions in natural and synthetic samples, we derive that such geometry represents a rare subsolidus evolution of pyroxenes quickly cooled from high temperatures. Sigmoidal shapes have also been found in apparently slowly cooled rocks (e.g. gabbros or monzodiorites), but it is not clear whether the specimens come from the chilled margin or not. The chemical composition and size of exsolution textures in synthetic pyroxenes closely match those of our chondritic pyroxene except for the coarser lamellae in RAG-20. For instance, Fig. 6.4 in Feuer et al. (1991) closely matches our Fig. 1c, and Fig. 2 in Feuer et al. (1989) strongly recalls Fig. 4 in Ferraris et al. (2002). We therefore conclude that the cooling rates of chondrules in H3 chondrites were not very different from synthetic runs cooled from 1350 °C to room temperature at a rate of about 8 °C hr^{-1}. Namely, microstructural features within primitive chondrites were established through quick cooling processes. Incipient annealing due to the mild thermometamorphic overprint recorded in H4 chondrites (e.g. Dodd 1981; Brearley and Jones 1998) may account for the thicker sigmoids observed in the Raguli pyroxenes.

Strained lattice parameters

Table 2 reports the lattice parameters for the different CPX–CLEN pairs. In the case of exsolved pigeonites (CPXs hosted within CLEN), the observed values for RAG-20, BFR-18, FR3-2 and FR3-1 chondrules are constant, with average values $a = 0.975$ nm, $c = 0.525$ nm and $\beta = 105.0°$ for CPX, and $a = 0.967$ nm, $c = 0.523$ nm and $\beta = 107.5°$ for CLEN; these do not differ much from those expected for similar compositions (i.e. close to $a = 0.975$ nm, $c = 0.524$ nm, $\beta = 106.0°$ for CPX and $a = 0.965$ nm, $c = 0.519$ nm, $\beta = 109.0°$ for CLEN) (Benna et al. 1990; Hugh-Jones 1997). Although unit cell dimensions were almost the same, we observed β angles 1° smaller than expected.

Exsolved CPXs consisting of CLEN domains hosted within a CPX matrix (i.e. BFR-6/1 and FR32-2) show greater discrepancies. In this case, average values ($a = 0.951$ nm, $c = 0.534$ nm and $\beta = 105.4°$ for CPX, and $a = 0.934$ nm, $c = 0.534$ nm and $\beta = 108.3°$ for CLEN) strongly deviate from values expected for similar compositions (e.g. $a = 0.975$ nm, $c = 0.524$, $\beta = 106.0°$ for CPX and $a = 0.962$, $c = 0.518$, $\beta = 108.8°$ for CLEN). In the latter case, the observed parameters are significantly shorter than the expected ones.

An intermediate case occurs for BFR-6/2, with a well-matching a parameter but anomalously long c vector.

In our opinion, these differences do not depend on biased determinations but are a real intrinsic feature of these nanometric pyroxenes. In particular, we suggest that they indicate the occurrence of important elastic strain. Strain effects arise between the domains connected through the systematically observed, totally coherent interfaces. In TEM images, strain produces contrast features within CLEN and CPX, such as the vertical ones in Fig. 1a. This issue has been previously addressed for cryptoperthitic feldspars; furthermore, it has also been briefly discussed in the case of coherently exsolved iron-free pyroxenes (Yund and Tullis 1983). Based on these previous experimental observations and relative theoretical models, we explain the anomalous lattice parameters in pyroxenes from sigmoidally exsolved chondrites as due to elastic strain within the CPX–CLEN exsolution texture. In agreement with Yund and Tullis (1983), we acknowledge that the

corresponding strain field is produced by elastic shear strain. As previously reported, exsolution textures range from well-defined sigmoids (RAG-20) to ill-defined features (FR32–2), approximately following the order of appearance in Table 1. The comparison with Table 2 reveals that lattice parameters are most strained where exsolution textures are most poorly defined.

Shear strain in exsolved pigeonite

The occurrence of shear strain in sigmoidally exsolved pyroxenes has been previously proposed on the basis of observed strained cell parameters. This indication is further supported by the direct-space observation of exsolution textures. Contours such as those shown in Fig. 1 immediately recall the sigmoidal shapes arising by simple shear stress in deformed rocks.

In contrast with structural geology and shock metamorphism, stress in the exsolved pyroxene crystals is caused by internal, and not external, forces. When planning this study, we deliberately excluded shock-deformed chondrites, so as to study the primary features of unequilibrated chondrites.

In particular, stress may originate within pyroxene when (100) low-pigeonite lamellae exsolve to '001' CLEN and '001' CPX at temperatures close to 850 °C. At this temperature, (100) low-temperature pigeonite lamellae (with lattice parameters $a = 0.9767$, $c = 0.5270$ nm and $\beta = 108.9°$; Tribaudino et al. 2002) transform into mismatching CLEN and CPX '001' lamellae. At 850 °C, the CLEN unit cell ($a = 0.9675$, $c = 0.5203$ nm and $\beta = 108.9°$; Hugh–Jones 1997) differs from the contracted PIG unit cell, but preserves the direction of lattice vectors (constant β angle). In contrast, CPX ($a = 0.9807$, $c = 0.5276$ nm and $\beta = 106.0°$; Benna et al. 1990) differs in both unit-cell size (expanded a translation) and lattice vector direction (β is 2.2° smaller). As a consequence, the combined effect of the a_{CPX} expansion and a_{CPX} clockwise rotation is that of pushing against CLEN, mostly close to the lamella termination. This joint effort activates the (100)[001] slip system by creating two opposite forces, which act in two different directions on the two lamella terminations and introduce a simple shear stress (depicted in Fig. 4). In reaction to simple shear stress, the lamellae relax and assume their final sigmoidal configuration.

An alternative model envisages the active role of OREN lamellae in triggering and shaping exsolutions in pigeonite. Iijima and Buseck (1975) have demonstrated that the introduction of an OREN lamella in clinopyroxene introduces a mismatch of the clinopyroxene cell edges parallel to [001] of $\sim c/10$ on opposite sides of the OREN lamellae. We believe that the mismatch could produce a shear stress parallel to [001] at the ortho-clinopyroxene interface. The resulting stress field would produce extension domains with sigmoidal shapes capable of accommodating excess calcium during cooling. The exsolution textures would thus form much like the sigmoidal en-echelon veins in brittle-ductile shear zones common in tectonites (e.g. Ramsay and Huber 1983). Upon further cooling, the sigmoids would acquire their final geometry due to the simple shear stress produced by the combined effect of the a_{CPX} expansion and a_{CPX} clockwise rotation, as detailed above. In other words, the highest the (100) OREN faults frequency, the higher the probability of sigmoidal exsolution. As a consequence, sigmoids should characterize faulted pyroxenes that inverted from high temperature polymorphs at $T > 1000$ °C upon rapid cooling.

Shear strain in exsolved augite

Shear stress may also explain the geometry of precipitates in augite. The shapes and arrangement of the CLEN precipitates in the BFR-6/1 augite (Fig. 2) are similar to those expected for pigeonitic lamellar precipitates in augite described in literature (e.g. Putnis 1992). On cooling, the high-temperature pigeonite lamellae ($C2/c$) invert to the low-temperature polymorph ($P2_1/c$) by decreasing the β angle by $\sim 1.5°$. To accommodate this change, the pigeonite lamellae undergo shear displacements on (100) stacking faults. This produces a stepped '001' interface, which retains its average orientation within the augite host. In contrast with this model, we observed that the precipitate is CLEN rather than pigeonite, probably in relation to a more extensive subsolidus ionic exchange between lamellae and host.

Conclusions

- Pyroxene in unequilibrated and poorly equilibrated H3 and H4 ordinary chondritic meteorites shows sigmoidal exsolution features. This morphology may be described in terms of the rotation of lamellae from '001' towards the '100' orientation.
- Sigmoidal precipitates are not peculiar to chondritic meteorites, but also occur in many terrestrial rocks and synthetic charges quickly cooled from high temperatures.
- In chondrules, sigmoidal exsolutions occur at temperatures lower than 1000 °C, more precisely within the 990–830 °C range, following the fast cooling path estimated by Ferraris et al. (2002) for unequilibrated chondrites.
- The sigmoidal morphology of the precipitates in pigeonite is produced by simple shear stress which promotes two opposite (100)[001] slip systems (i.e. through the '001' interface rotation due to lattice misfit) within pairs of (100) OREN lamellae. Alternatively, the introduction of pairs of OREN lamellae in clinopyroxene plays an earlier role in triggering and shaping exsolutions in pigeonite by introducing shear stress parallel to [001] at the ortho–clinopyroxene interface; shear stress produces extension

domains with sigmoidal shapes in clinopyroxene, which can preferentially accommodate excess calcium during cooling.
– The stepped morphologies of the CLEN precipitates in augite are explained by shear displacements along (100) stacking faults (1.8 nm, OREN lamellae), as described in literature for pigeonite '001' lamellae in augite (e.g. Putnis 1992).
– As (100) OREN lamellae frequently occur within chondritic pyroxenes due to inversion from high temperature polymorphs upon rapid cooling, sigmoids may be more common in chondrites.

Acknowledgements We thank Dr. S. Weinbruch and an anonymous referee for the useful comments, and Prof. A. Putnis for editorial assistance.

References

Benna P, Tribaudino M, Zanini G, Bruno E (1990) The crystal structure of $Ca_{0.8}Mg_{1.2}Si_2O_6$ clinopyroxene ($Di_{80}En_{20}$) at $T = -130$, 25, 400 and 700 °C. Z Kristallogn 192: 183–199

Brearley AJ, Jones RH (1998) Chondritic meteorites. In: Papike JJ (ed) Planetary materials. Reviews in Mineralogy, vol 36. Mineralogical Society of America, Washington DC pp 3–1 to 3–398

Dodd RT (1981) Meteorites: a petrologic-chemical synthesis. Cambridge University Press, Cambridge, UK, pp 368

Ferraris C, Folco L, Mellini M (2002) Chondrule thermal history from unequilibrated H chondrites: a transmission and analytical electron microscopy study. Meteorit Planet Sci 37: 1299–1322

Feuer H, Schröpfer L, Fuess H, Jefferson DA (1989) High-resolution transmission electron microscopy study of exsolution in synthetic pigeonite. Eur J Mineral 1: 507–516

Feuer H, Schröpfer L, Fuess H (1991) Microstructures and thermal behaviour of igneous pyroxenes. In: Voll G, Töpel J, Pattison DRM, Seifert F (eds) Equilibrium and kinetics in contact metamorphism. Springer, Berlin Heidelberg New York, pp 105–120

Folco L (1997) Pyroxene thermometry in chondritic meteorites. PhD Dissertation, The Open University, Milton Keynes, UK, pp 188

Folco L, Mellini M, Pillinger CT (1996) Unshocked equilibrated H-chondrites: a common low-temperature record from orthopyroxene iron-magnesium ordering. Meteorit Planet Sci 31: 388–393

Geiger CA (2001) Solid solutions in silicate and oxide systems, Eötvös University Press, Budapest, Hungary, pp 465

Gooding JL, Keil K (1981) Relative abundances of chondrule primary textural types in ordinary chondrites and their bearing on conditions of chondrules formation. Meteoritics 16: 17–43

Grossman JN, Rubin AE, Nagahara H, King EA (1988) Properties of chondrules. In: Kerridge JF, Matthews MS (eds) Meteorites and the early solar system. University of Arizona Press, Tucson, Arizona, USA, pp 619–659

Hugh–Jones D (1997) Thermal expansion of $MgSiO_3$ and $FeSiO_3$ ortho- and clinopyroxenes. Am Mineral 82: 689–696

Iijima S, Buseck PR (1975) High resolution electron microscopy of enstatite. I: Twinning, polymorphism, and polytypism. Am Mineral 60: 758–770

Kitamura M, Yasuda M, Morimoto N (1981a) Morphology change of exsolution lamellae of pigeonite in Bushveld augite an electron microscopic observation. Proc Jap Acad 57: 183–187

Kitamura M, Yasuda M, Morimoto N (1981b) A study of fine textures of Bushveld augite by 200 kV analytical electron microscope. Bull Minéral 104: 278–284

Lindsley DH (1983) Pyroxene thermometry. Am Mineral 68: 477–493

McCallister RH (1978) The coarsening kinetics associated with exsolution in an iron-free clinopyroxene. Contrib Mineral Petrol 65: 327–331

Moore KT, Elbert DE, Veblen DR (2001a) Energy-filtered transmission electron microscopy (EFTEM) of intergrown pyroxenes. Am Mineral 86: 814–825

Moore KT, Veblen DR, Howe JM (2001b) Calcium segregation at antiphase boundaries in pigeonite. Am Mineral 86: 1314–1318

Müller WF (1993) Thermal and deformation history of the Shergotty meteorite deduced from clinopyroxene microstructure. Geoch Cosmoch Acta 57: 4311–4322.

Putnis A (1992) Introduction to mineral sciences. Cambridge University Press, Cambridge, UK, pp 457

Ramsay JG, Huber MI (1987) Modern structural geology, vol 2. Folds and fractures. Academic Press, London pp 700

Ried H, Fuess H (1986) Lamellar exsolution systems in clinopyroxene. Transmission electron microscope observations. Phys Chem Miner 13: 113–118

Rietmeijer FJM, Champness PE (1982) Exsolution structures in calcic pyroxenes from the Bjerkreim-Sokndal lopolith, SW Norway. Mineral Mag 45: 11–24

Robinson P, Jaffe HW, Ross M, Klein C (1971) Orientation of exsolution lamellae in clinopyroxenes and clinoamphiboles: consideration of optimal phase boundaries. Am Mineral 56: 909–939

Robinson P, Ross M, Nord GL Jr, Smyth JR, Jaffe HW (1977) Exsolution lamellae in augite and pigeonite: fossil indicators of lattice parameters at high temperature and pressure. Am Mineral 62: 857–873

Takeda H, Mori H, Ishii T, Miyamoto M (1981) Thermal and impact histories of pyroxenes in lunar eucrite-like gabbros and eucrites. Proc Lunar Planet Sci 12(B): 1297–1313

Tribaudino M, Nestola F, Cámara F, Domeneghetti MC (2002) The high-temperature $P2_1/c$-$C2/c$ phase transition in Fe-free pyroxene ($Ca_{0.15}Mg_{1.85}Si_2O_6$): structural and thermodynamic behavior. Am Mineral 87: 648–657

Yund RA, Tullis J (1983) Strained cell parameters for coherent lamellae in alkali feldspars and iron-free pyroxenes. N Jb Mineral Mh 22–34

Weinbruch S, Müller W, Hewins RH (2001) A transmission electron microscope study of exsolution and coarsening in iron-bearing clinopyroxene from synthetic analogues of chondrules. Meteorit Planet Sci 36: 1237–1248